



# Defining the target prior to prostate fusion biopsy: the effect of MRI reporting on cancer detection

Niklas Westhoff<sup>1</sup> · Fabian Siegel<sup>1</sup> · Christian Peter<sup>1</sup> · Svetlana Hetjens<sup>2</sup> · Stefan Porubsky<sup>3</sup> · Thomas Martini<sup>4</sup> · Jost von Hardenberg<sup>1</sup> · Maurice Stephan Michel<sup>1</sup> · Johannes Budjan<sup>5</sup> · Manuel Ritter<sup>1</sup>

Received: 28 April 2018 / Accepted: 28 June 2018 / Published online: 2 July 2018  
© Springer-Verlag GmbH Germany, part of Springer Nature 2018

## Abstract

**Purpose** Definition of targets in multiparametric MRI (mpMRI) prior to MRI/TRUS fusion prostate biopsy either by urologist or radiologist, as a prose report or by illustration is crucial for accurate targeted biopsies (TB). The objective was to analyze the effect of MRI reporting on target definition and cancer detection.

**Methods** 202 patients underwent MRI/TRUS fusion biopsy with Artemis™ (Eigen, USA). mpMRI results were submitted in written form to urologists, who marked the targets in the proprietary software. An expert urologist reviewed and marked mpMRI targets blinded to biopsy data. We compared number, localization and volume of targets between the observers and analyzed whether variations impaired TB results by bivariate and logistic regression models.

**Results** Interobserver variability was moderate regarding number and low regarding localization of targets. Urologists overestimated target volumes significantly compared to radiologists ( $p = 0.045$ ) and matching target volume between both observers was only 43.9%. Overall cancer detection rate was 69.8 and 52.0% by TB. A higher matching target volume was a significant predictor of cancer in TB ( $p < 0.001$ ). Logistic regression revealed prostate volume and PI-RADS as independent predictors. Defining targets in incorrect T2w slices in the cranio-caudal axis are one presumable reason for missing cancer in TB.

**Conclusions** A high concordance of the target definition between radiologist and urologist is mandatory for accurate TB. Optimized ROI definition is recommended to improve TB results, preferably as contouring in MRI sequences by the radiologist or, if not feasible, by precise MRI reports including specific localization in sequence and slice as well as an illustration. High prostate volume and low PI-RADS score have to be considered as limiting factors for target definition.

**Keywords** Prostatic neoplasms · Multiparametric MRI · Biopsy · Fusion · Interobserver variability

Johannes Budjan and Manuel Ritter contributed equally to this work.

**Electronic supplementary material** The online version of this article (<https://doi.org/10.1007/s00345-018-2400-x>) contains supplementary material, which is available to authorized users.

✉ Niklas Westhoff  
niklas.westhoff@medma.uni-heidelberg.de

<sup>1</sup> Department of Urology, University Medical Center Mannheim, Medical Faculty Mannheim, University of Heidelberg, Theodor-Kutzer-Ufer 1-3, 68167 Mannheim, Germany

<sup>2</sup> Institute of Medical Statistics and Biometry, University Medical Center Mannheim, Medical Faculty Mannheim, University of Heidelberg, Theodor-Kutzer-Ufer 1-3, 68167 Mannheim, Germany

## Introduction

Multiparametric MRI enriches prostate cancer diagnostics, providing visibility of suspicious tumor lesions and paving the way for TB and focal treatment. MRI/ultrasound fusion-guided prostate biopsy leads to increasing detection

<sup>3</sup> Department of Pathology, University Medical Center Mannheim, Medical Faculty Mannheim, University of Heidelberg, Theodor-Kutzer-Ufer 1-3, 68167 Mannheim, Germany

<sup>4</sup> Department of Urology, University Medical Center Ulm, Prittwitzstraße 43, 89075 Ulm, Germany

<sup>5</sup> Institute of Clinical Radiology and Nuclear Medicine, University Medical Center Mannheim, Medical Faculty Mannheim, University of Heidelberg, Theodor-Kutzer-Ufer 1-3, 68167 Mannheim, Germany

rates of clinically significant prostate cancer when compared to systematic biopsy (SB) [1, 2]. Application of the Prostate Imaging Reporting and Data System (PI-RADS) in 2012 and its updated version in 2015 allowed standardized mpMRI interpretation among different radiologists [3, 4]. Thus, specificity and sensitivity of mpMRI are reported to be up to 88 and 89%, respectively [5, 6]. Fusion biopsy is recommended by current guidelines for repeat biopsies in primary diagnostics and active surveillance protocols [7, 8]. Usage in biopsy-naïve patients is still under debate, but reveals promising results in recent randomized trials [7–9]. The increasing demand for fusion biopsies and the feasibility to perform them either with cognitive or software-based image fusion warrants MRI/ultrasound-guided biopsies be distributed evenly across healthcare providers rather than limited to a few experts in high-volume centers.

However, prostate fusion biopsy is more complex than regular SB, involving multiple steps that affect accuracy, such as image registration, precise ultrasound navigation, and biopsy sampling. Large series comparing TB and SB demonstrated that only the combination of both techniques yields the best diagnostic accuracy [2, 10]. There is a substantial risk of missing significant cancers by TB, demonstrated by the negative predictive values ranging from 0.65 to 0.94 [11].

When evaluating optimization of fusion biopsy, most studies focus on adequate acquisition of mpMRI, image interpretation, mpMRI/ultrasound fusion techniques, and the accuracy of biopsy sampling [1, 12–15]. In this study, we focus on a key step that is crucial for precise sampling of the region of interest (ROI) and is of utmost importance for the workflow in clinical and outpatient settings: reporting on MRI results varies greatly between radiologists as findings are provided either in a prose text, illustrated approximately on a sector map or delineated in the MRI sequence itself. It is common that urologists have to localize the target lesion in mpMRI only based on the description in written form without any illustration. This requires the urologist to be highly experienced in mpMRI interpretation. Therefore, we compared mpMRI target definitions by radiologists and urologists prior to MRI/TRUS fusion biopsy and analyzed whether differences affect tumor detection.

## Materials and methods

### Patients

Reasons for MRI/TRUS fusion biopsy comprised elevated PSA levels, abnormal DRE findings or confirmed cancer, either undergoing active surveillance or before focal HIFU treatment. Inclusion criteria were at least one suspicious lesion on mpMRI and the presence of a mpMRI report in a

written form. We excluded 7 patients without a suspicious lesion on control mpMRI after focal HIFU therapy.

### Multiparametric MRI and MRI/TRUS fusion biopsy

The whole-body 3.0 Tesla scanners Magnetom Skyra and Trio (Siemens Healthineers, Erlangen, Germany) were used for mpMRI in clinical routine. The acquisition protocol included high resolution T2-weighted sequences in transverse, coronal, and sagittal planes, diffusion-weighted imaging ( $b$  values of 50,400,800 s/mm<sup>2</sup>, additional  $b$  value of 2000 s/mm<sup>2</sup> for Skyra) and dynamic contrast-enhanced (DCE) T1-weighted perfusion sequences.

All initial mpMRI analyses were routinely performed by urologists and supervised by senior radiologists of at least 4 years of expertise in prostate MRI reading ( $n=21$  radiologists, this group was defined as “radiologist A”). Regions of interest (ROI) were classified according to PI-RADS classification v1 or v2 or as “suspicious”, depending on the time of acquisition. The reports were submitted to urologists in written form without marking the ROIs in MRI images. A standard written report included information on the ROI localization in T2w transversal sequence according to the PI-RADS sector map or by an anatomical description, results of diffusion-weighted imaging and DCE, and lymph node or bone metastasis.

The biopsy platform Artemis™ (Eigen, California, USA) was used for MRI/TRUS fusion-guided prostate biopsies. After import of the mpMRI raw data, surgeons used the proprietary ProFuse™ software (version 3.0.7.1) to mark the prostate contours in various slices. An automatic interpolation completed the contouring before a manual redefining was possible. Subsequently, all regions of interest were marked by an exact contouring in the T2w sequence (Fig. 1). Afterwards, TB followed by 12-core SB was performed as previously described [16, 17].

### Image processing

One expert urologist with more than 4 years training in prostate mpMRI reading (J.B., defined as “radiologist B”) resurveyed all 202 mpMRI images and contoured the lesion in T2w sequences based on the previous MRI report and all available sequences of the respective study using the Osirix software (Pixmeo SARL, Swiss). Radiologist B was blinded to the biopsy results. A lesion was always marked in all the transverse T2w slices where it was identifiable.

We compared the area of the ROIs marked by the radiologist and urologist by a software algorithm that recognized each contour. ROI volumes were calculated by addition of the voxel volume of each slice. Subsequently, we compared the ROI contouring and calculated the matching ROI volume

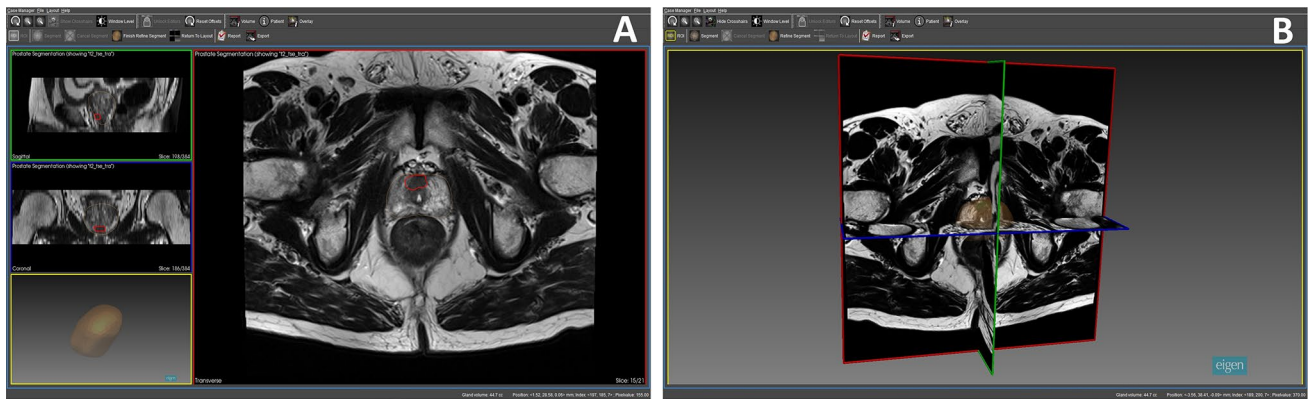


**Fig. 1** Contouring the ROI in the ProFuse Software (Eigen, USA) prior to image fusion. **a** Delineation of the prostate and ROI (red) in transverse T2w sequences. **b** 3D model of the prostate to visualize correct delineation and ROI definition

of both observers (defined as common ROI volume = cROI volume) (Fig. 2).

In addition, we evaluated whether contouring a ROI in the wrong MRI slice (i.e., shifted in the cranio-caudal axis) impaired the cROI volume. Therefore, we merged all transverse MRI slices irrespective of slice order where radiologist B and urologist marked the ROI. We thus created a projection of the marked ROIs which ignored any cranio-caudal error in ROI contouring. The resulting cROI volumes were calculated (Fig. 3).

### Statistical analysis

Cohen's Kappa statistic was used for calculation of inter-observer variability between radiologist A, radiologist B,

and urologists. Wilcoxon rank sum test was used for statistical comparison of the median ROI volumes. We calculated intraclass correlation coefficient (ICC) to evaluate variance of the volume measurements. Potential predictors for a cancer-positive TB were evaluated by bivariate analysis. For approximately normally distributed data, two sample *t* tests have been used to compare the mean values of two groups. For skewed variables, Mann–Whitney *U* tests were performed instead. For the comparison of qualitative parameters, Chi square test or Fisher's exact test have been applied. Significant variables were included for a multivariate logistic regression model to determine their independent prognostic value. Analyses were performed using SAS<sup>®</sup> 9.3 software and statistical significance was set at  $p < 0.05$ .

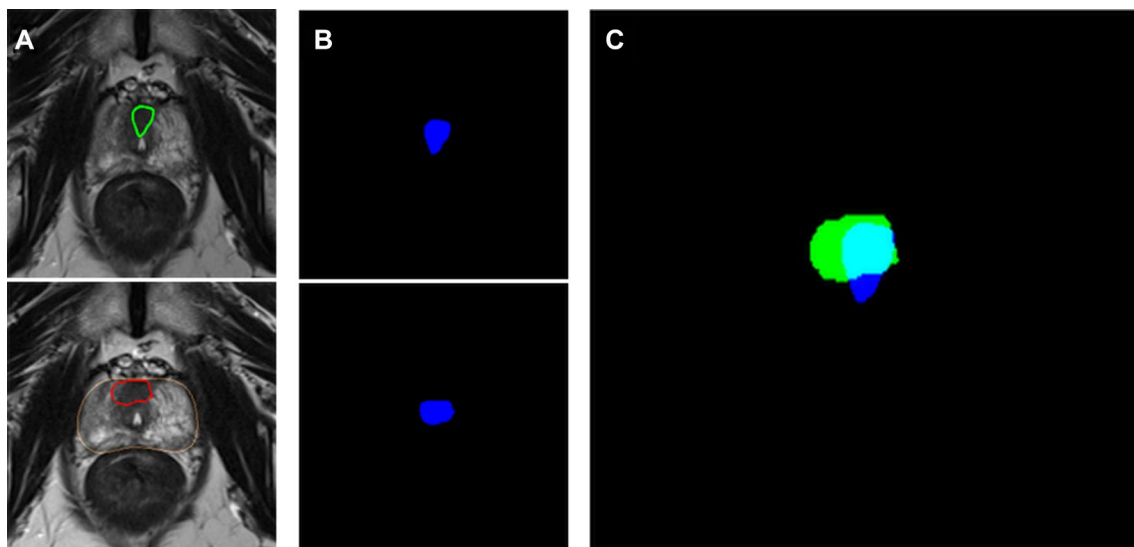


**Fig. 2** T2w sequences with ROI marked by the radiologist (a) and urologist (b). Automated extraction of ROI contours (c) was followed by merging of the MRI sequences (d). The turquoise overlapping part of both ROIs represents the common fraction

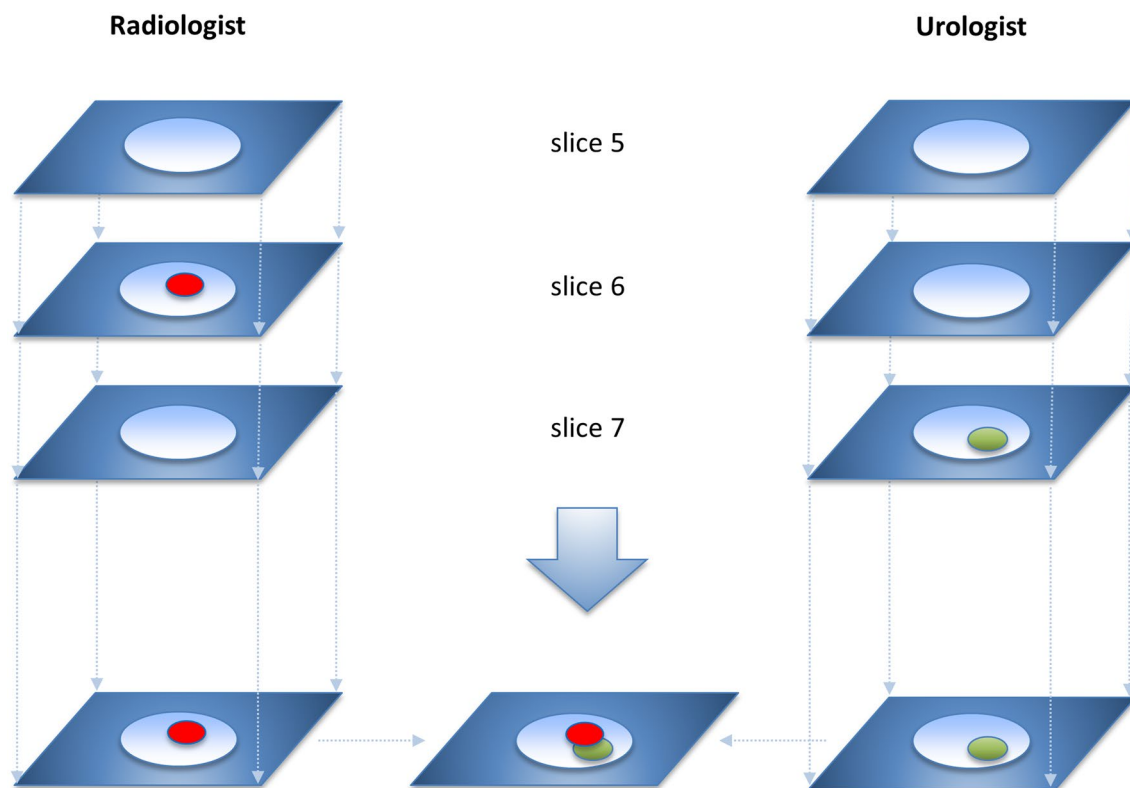


**Fig. 3** Schematic description of the merging process for patients without any cROI volume: When ROIs were defined in different T2w slices, all MRI images were merged independently of the slice. Light

oval: prostate, red oval: ROI defined by radiologist, green oval: ROI defined by urologist

## Results

### Patient characteristics

In total, 202 patients received an mpMRI of the prostate and a consecutive MRI/TRUS fusion biopsy between December 2014 and December 2016. Of those, 46.5% received re-biopsy after a prior negative biopsy, 24.3% had a prior confirmed cancer, and 29.2% were biopsy-naïve. Patient characteristics are provided in Online Resource 1. Five patients with a suspicious control mpMRI 12 month after HIFU therapy were also included. For the comparison of ROI volumes, the 165 patients with an equal number of ROIs per evaluation were included. In 157 of the 165 patients, the ROIs or part of them were marked in the same prostate lobe and zone by both observers. In 7 patients, the prostate zone and in one patient the lobe were different. Additionally, for bi- and multivariate analysis, another 11 patients were excluded because their suspicious lesion was not classified according to PI-RADS (6 patients with proven cancer in TB and 5 patients without).

### Multiparametric MRI results and definition of ROIs

The mpMRI analysis by radiologist A revealed 239 lesions in 202 patients, with a median of one lesion per patient (range 1–3). In more than a third of all patients (34.2%), the index lesion was classified as PI-RADS 3 (Table 1). Index lesions had a median diameter of 12 mm (5–45 mm). We compared if mpMRI interpretation differed between all observers. Urologists contoured the highest number of ROIs compared to radiologist A and radiologist B (261 vs. 239 vs. 223). This resulted in a substantial interobserver variability ( $\kappa = 0.41–0.65$ ). In contrast, the localization of ROIs according to the PI-RADS sector maps differed less between the three observers ( $\kappa = 0.76–0.84$ ) (Table 2) [4].

Urologists marked significantly larger median ROI volumes than radiologists in the 165 patients with an equal number of ROIs per evaluation ( $p = 0.045$ ). The median cROI volume of urologist and radiologist B was  $0.24 \text{ cm}^3$  ( $0–11.44 \text{ cm}^3$ ), which represents a median fraction of

**Table 1** Results of mpMRI and MRI/TRUS fusion biopsy ( $n=202$  patients)

Variable	Value
<b>mpMRI results</b>	
Number of ROIs ( $n, \%$ )	
Total	239
Per patient (median, range)	1 (1–3)
$n = 1$	170 (84.16)
$n = 2$	27 (13.37)
$n = 3$	5 (2.48)
PI-RADS index lesion* ( $n, \%$ )	
1	1 (0.50)
2	8 (3.96)
3	69 (34.16)
4	56 (27.72)
5	52 (25.74)
No PI-RADS	14 (6.93)
<b>Biopsy results</b>	
Overall cancer detection ( $n, \%$ )	141/202 (69.80)
Cancer detected by TB ( $n, \%$ )	
Per patient	105/202 (51.98)
Per lesion	124/239 (51.88)
Cancer detected by SB ( $n, \%$ )	129/202 (63.86)
Number of cores obtained per lesion (median, range)	2 (1–8)
Number of SB cores obtained per patient (all patients)	12
<b>Gleason scores</b>	
3 + 3	70 (34.65)
3 + 4	39 (19.31)
4 + 3	26 (12.87)
4 + 4	2 (0.01)
4 + 5	1 (0.01)
5 + 4	3 (0.02)
5 + 5	0 (0)

TB target biopsy, SB systematic biopsy

\*Lesion with highest PI-RADS score in case of > 1 lesion

**Table 2** Agreement of ROI count and localization between three observers using Cohen’s kappa coefficient ( $\kappa$ )

Variable	rA – rB	rA – U	rB – U
Number of ROIs	0.54	0.65	0.41
ROI localization	0.84	0.84	0.76

rA first reading radiologist, rB second reading radiologist, U urologists

43.86% of the radiologists’ ROI volume (Fig. 4). Intraclass correlation coefficient was 0.84 for variances of volume measurements.

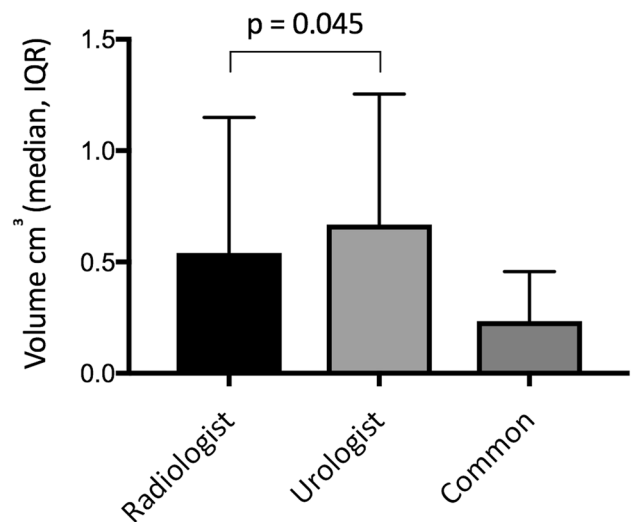


**Fig. 4** Median ROI volumes by radiologist and urologist were significantly different. A median fraction of 43.86% of the radiologists’ ROI volume matched with the urologists’ volume (cROI volume)

**Biopsy results**

In the 165 patients, the overall cancer detection of combined TB (a median of 2 TB per ROI; range 1–8) and 12-core SB was 68.5%. TB was positive in 52.0 and 51.9% in a per patient- and a per lesion-based analysis, respectively (Table 1).

In the subgroup analysis of 154 patients with either a positive or negative TB and classification by PI-RADS (Table 3), the cROI volume was higher in the group of positive TB. Bivariate analysis revealed ROI volume of the radiologist, cROI volume, prostate volume and PI-RADS score as significant predictive variables for a cancer-positive biopsy. In a multivariate logistic regression model, a smaller prostate volume and higher PI-RADS score remained independent factors (Table 4).

SB revealed cancer in 63.9%. In 67.8% of the 90 cancer-positive ROIs, at least one SB sample was positive in the corresponding prostate sextant. The systematically obtained cancer-positive biopsy core within this sextant was a significant predictor of a positive TB in bi- and multivariate analysis ( $p \leq 0.001$ ) (Online Resource 2).

**Relevance of MRI image slice**

Target definition differed entirely between the radiologist and urologist in 38 patients (23%) and no cROI volume was measurable. As selecting the wrong T2w slice for target localization could be a potential bias in these patients, we merged all slices where radiologist and urologist marked the ROI. This resulted in an increased cROI

**Table 3** Patient characteristics separated by target biopsy result

	Target biopsy positive ( <i>n</i> = 76)	Target biopsy negative ( <i>n</i> = 77)
ROI volume radiologist, cm <sup>3</sup> (median, range)	0.69 (0.11–13.80)	0.44 (0.09–6.70)
ROI volume urologist, cm <sup>3</sup> (median, range)	0.74 (0.08–24.45)	0.57 (0.10–7.69)
cROI volume*, cm <sup>3</sup> (median, range)	0.29 (0–11.44)	0.14 (0–6.31)
PSA, ng/ml (median, range)	9.4 (2.46–88)	8.14 (0.66–55)
Prostate volume, cm <sup>3</sup> (median, range)	40 (18–113)	60 (15–250)
ROIs (n) (median, range)	1 (1–3)	1 (1–2)
PI-RADS index lesion (median, range)	4 (3–5)	3 (1–5)
Biopsy status ( <i>n</i> , %)		
Biopsy-naïve	30 (39.47)	14 (18.18)
Prior negative	36 (47.37)	41 (53.25)
Prior positive	10 (13.16)	22 (28.57)
Target biopsy cores per lesion (median, range)	3 (2–6)	2 (1–8)
Positive SB in ≥ 1 positive ROI sextant (median, range)	53 (69.74)	12 (15.58)

*cROI* common ROI volume

**Table 4** Bivariate and multivariate analysis for cancer-positive targeted biopsy

	Bivariate analysis		
	<i>p</i>		
ROI volume radiologist	<0.001		
ROI volume urologist	0.075		
cROI volume	<0.001		
PSA	0.629		
Prostate volume	0.003		
Number of ROIs	0.130		
PI-RADS index lesion	<0.001		
Target biopsy cores per lesion	0.276		
	Logistic regression		
	Odds ratio	95% CI	<i>p</i>
ROI volume radiologist	1.72	0.55–5.35	0.349
ROI volume urologist	1.09	0.58–2.07	0.786
cROI volume	1.63	0.2–13.64	0.650
Prostate volume	0.98	0.96–1.0	0.025
PI-RADS index lesion	2.41	1.36–4.25	0.003

volume fraction of 67.1% and reduced the number of patients without any cROI fraction to 10 patients (6.1%). TB was positive in 8 of 38 patients (21.1%), whereas SB was positive in 19/38 patients (50%). Of those, four cancers were missed by TB but found by at least one SB core in the corresponding prostate sextant (Online Resource 3).

## Discussion

The fundamental prerequisite prior to MRI/TRUS fusion and targeted biopsy is the exact localization of the MRI visible lesion. ESUR guidelines recommend “preferably using a structured reporting scheme”, that includes PI-RADS score, localization and extraprostatic extent, as well

as incidental findings [3, 4]. However, there is uncertainty on how to transmit MRI reports to urologists and whether radiologists or urologists should mark the target in MRI sequences [18]. Therefore, this study compared ROI definitions by radiologists and urologists and determined the effect of different observers on prostate cancer detection.

We observed that interobserver variability between the first reading radiologists, the resurveying radiologist and the urologists was higher for the total number of marked ROIs than for localization according to the sector map. Urologists marked more ROIs compared to the MRI report and to radiologist B, which is likely due to their interpretation of additional areas that appear suspicious but do not fulfill all PI-RADS criteria. In addition, correspondence with various radiologists immediately before biopsy to confirm correct ROI localization could have led to different reading results. It was shown that MRI interpretation and biopsy sampling underlie a learning curve [19, 20]. This is a further explanation for both variances between urologists and radiologists, and between radiologist A and B.

Target definition not only differed in terms of number and localization, but also in volume. Urologists tend to mark larger volumes. It is conceivable that this is justified by a safety strategy to avoid undersampling of the suspicious region. Underestimation of tumor size in mpMRI images was previously demonstrated, particularly in the context of focal therapies, leading to incomplete tumor ablation [21]. But, marking an oversized ROI around a small tumor might result in missing the tumor by inaccurate biopsy sampling. Since ROI volume data was not normally distributed, we used bar charts for comparison instead of a Bland–Altman plot. ICC (0.84) revealed that measurement variance certainly was based on observer disagreement.

When comparing cROI volume between the different observers with regard to biopsy result, the subgroup of patients with a TB positive for cancer had a higher conformity between radiologist and urologist. Vice versa, discrepancies in target definitions appear to impact cancer detection. Bivariate analysis confirmed the cROI volume as a statistically significant predictive variable for a positive biopsy result ( $p < 0.001$ ). However, in our cohort, only 43.9% of the urologists' ROI volumes matched with those of the radiologists. The most likely reason is a misjudgment of morphological variances or distinct signal intensities appearing like suspicious ROIs but lacking malignancy criteria. Hence, it is likely that in inconclusive MRI results, neither a written nor oral description of the ROI would adequately enable an unversed urologist to define the “true” ROI. We further hypothesized that MRI reports frequently lack information on MRI series and slices for ROI localization. Subsequently, if the urologist marks the ROI in an incorrect slice, this could affect hitting the target. We merged MRI images independently of the T2w slice and found that

the cROI volume could be considerably increased. Thus, ROIs had been marked similarly in transverse planes but were located differently along the cranio-caudal axis. In the patients without any cROI volume, this could have resulted in cancers detected by SB in the same prostate sextant that were missed by TB in four cases.

We performed a multivariate logistic regression analysis in which, in contrast to bivariate analysis, large prostate volumes, and a lower PI-RADS score were the only independent predictors of positive biopsy results. To further investigate why cROI volumes remained statistically insignificant, we evaluated whether tumor extents were higher than expected in mpMRI and thereby more likely to be detected, and assumed a positive SB in the same prostate region as a surrogate marker. In more than two-thirds of all ROIs where TB was positive, at least one SB core in the same region was positive. We concluded that, in these patients, precise ROI definition and TB played a minor part, since large tumor volumes allowed detection by SB. A different explanation is that large prostate volumes and lower PI-RADS scores complicate target localization and selection for both radiologists and urologists. Previous studies demonstrated increasing detection rates in lower prostate volumes and for lesions with higher PI-RADS scores [10, 22].

These results are limited due to the lack of histopathological alignment as a reference for appropriate ROI definition. In prostatectomy specimens, the exact tumor localization could be compared to the assumed ones in mpMRI. However, we performed an extensive image analysis and correlation to clinical results, proving the need for optimization of MRI reporting in the future. In addition, results from both the MRI reports and contouring of the targets, originate from different observers. Their variety of expertise may lead to a bias, but this study intended to represent the clinical routine where typically MRI reporting and biopsy sampling are not restricted to the hands of single experts.

## Conclusion

ROI definition by urologists based on a prose MRI report is common prior to MRI/ultrasound fusion biopsy. A comparison of ROI definition in the original MRI report by a reviewing urologist and by an urologist revealed remarkable discrepancy in MRI contouring. The impact of an accurate target definition on cancer detection via biopsy was demonstrated by a higher conformity between the observers in targets positive for cancer. Thus, MRI reporting in written form might lack detailed information for urologists without expert knowledge. Accuracy of targeted biopsies would profit from ROI contouring in MRI sequences by the radiologist. If not feasible, improved MRI reporting should include specific information on ROI localization in sequence and

slice accompanied by an illustration. However, large prostate volumes and lower PI-RADS scores have to be considered as most limiting variables affecting biopsy results.

**Author contributions** NW: project development, data collection, data analysis, manuscript writing. FPS: project development, data analysis, manuscript editing. CP: data collection, manuscript editing. SH: data analysis, manuscript editing. SP: data collection, manuscript editing. TM: manuscript editing. JvH: manuscript editing. MSM: manuscript editing. JB: data collection, manuscript editing. MR: project development, manuscript editing.

## Compliance with ethical standards

**Conflict of interest** The authors declare that they have no conflict of interest.

**Ethical standards** For this type of study formal consent is not required.

## References

- Bjurlin MA, Meng X, Le Nobin J, Wysock JS, Lepor H, Rosenkrantz AB, Taneja SS (2014) Optimization of prostate biopsy: the role of magnetic resonance imaging targeted biopsy in detection, localization and risk assessment. *J Urol* 192(3):648–658. <https://doi.org/10.1016/j.juro.2014.03.117>
- Siddiqui MM, Rais-Bahrami S, Turkbey B, George AK, Rothwax J, Shakir N, Okoro C, Raskolnikov D, Parnes HL, Linehan WM, Merino MJ, Simon RM, Choyke PL, Wood BJ, Pinto PA (2015) Comparison of MR/ultrasound fusion-guided biopsy with ultrasound-guided biopsy for the diagnosis of prostate cancer. *JAMA* 313(4):390–397. <https://doi.org/10.1001/jama.2014.17942>
- Weinreb JC, Barentsz JO, Choyke PL, Cornud F, Haider MA, Macura KJ, Margolis D, Schnall MD, Shtern F, Tempny CM, Thoeny HC, Verma S (2016) PI-RADS prostate imaging—reporting and data system: 2015, Version 2. *Eur Urol* 69(1):16–40. <https://doi.org/10.1016/j.eururo.2015.08.052>
- Barentsz JO, Richenberg J, Clements R, Choyke P, Verma S, Villeirs G, Rouviere O, Logager V, Futterer JJ, European Society of Urogenital R (2012) ESUR prostate MR guidelines 2012. *Eur Radiol* 22(4):746–757. <https://doi.org/10.1007/s00330-011-2377-y>
- Woo S, Suh CH, Kim SY, Cho JY, Kim SH (2017) Diagnostic performance of prostate imaging reporting and data system version 2 for detection of prostate cancer: a systematic review and diagnostic meta-analysis. *Eur Urol*. <https://doi.org/10.1016/j.eururo.2017.01.042>
- Hamoen EH, de Rooij M, Witjes JA, Barentsz JO, Rovers MM (2015) Use of the prostate imaging reporting and data system (PI-RADS) for prostate cancer detection with multiparametric magnetic resonance imaging: a diagnostic meta-analysis. *Eur Urol* 67(6):1112–1121. <https://doi.org/10.1016/j.eururo.2014.10.033>
- European Association of Urology (EAU) (2017) Guidelines on prostate cancer. <http://uroweb.org/guideline/prostate-cancer/>. Accessed 8 Apr 2018
- Deutsche Gesellschaft für Urologie e.V. (DGU) (2018) Interdisziplinäre Leitlinie der Qualität S3 zur Früherkennung, Diagnose und Therapie der verschiedenen Stadien des Prostatakarzinoms. [https://www.awmf.org/uploads/tx\\_szleitlinien/043-022OLI\\_S3\\_Prostatakarzinom\\_2018-04.pdf](https://www.awmf.org/uploads/tx_szleitlinien/043-022OLI_S3_Prostatakarzinom_2018-04.pdf). Accessed 8 Apr 2018
- Ahmed HU, El-Shater Bosaily A, Brown LC, Gabe R, Kaplan R, Parmar MK, Collaco-Moraes Y, Ward K, Hindley RG, Freeman A, Kirkham AP, Oldroyd R, Parker C, Emberton M, Group PS (2017) Diagnostic accuracy of multi-parametric MRI and TRUS biopsy in prostate cancer (PROMIS): a paired validating confirmatory study. *Lancet* 389(10071):815–822. [https://doi.org/10.1016/s0140-6736\(16\)32401-1](https://doi.org/10.1016/s0140-6736(16)32401-1)
- Filson CP, Natarajan S, Margolis DJ, Huang J, Lieu P, Dorey FJ, Reiter RE, Marks LS (2016) Prostate cancer detection with magnetic resonance-ultrasound fusion biopsy: the role of systematic and targeted biopsies. *Cancer* 122(6):884–892. <https://doi.org/10.1002/cncr.29874>
- de Rooij M, Hamoen EH, Futterer JJ, Barentsz JO, Rovers MM (2014) Accuracy of multiparametric MRI for prostate cancer detection: a meta-analysis. *AJR Am J Roentgenol* 202(2):343–351. <https://doi.org/10.2214/AJR.13.11046>
- Shin T, Smyth TB, Ukimura O, Ahmadi N, de Castro Abreu AL, Ohe C, Oishi M, Mimata H, Gill IS (2017) Diagnostic accuracy of a five-point Likert scoring system for magnetic resonance imaging (MRI) evaluated according to results of MRI/ultrasonography image-fusion targeted biopsy of the prostate. *BJU Int*. <https://doi.org/10.1111/bju.13972>
- Wysock JS, Rosenkrantz AB, Huang WC, Stifelman MD, Lepor H, Deng FM, Melamed J, Taneja SS (2014) A prospective, blinded comparison of magnetic resonance (MR) imaging-ultrasound fusion and visual estimation in the performance of MR-targeted prostate biopsy: the PROFUS trial. *Eur Urol* 66(2):343–351. <https://doi.org/10.1016/j.eururo.2013.10.048>
- Delongchamps NB, Peyromaure M, Schull A, Beuvon F, Bouazza N, Flam T, Zerbib M, Muradyan N, Legman P, Cornud F (2013) Prebiopsy magnetic resonance imaging and prostate cancer detection: comparison of random and targeted biopsies. *J Urol* 189(2):493–499. <https://doi.org/10.1016/j.juro.2012.08.195>
- Hausmann D, Aksoz N, von Hardenberg J, Martini T, Westhoff N, Buettner S, Schoenberg SO, Riffel P (2017) Prostate cancer detection among readers with different degree of experience using ultra-high b-value diffusion-weighted Imaging: is a non-contrast protocol sufficient to detect significant cancer? *Eur Radiol*. <https://doi.org/10.1007/s00330-017-5004-8>
- Natarajan S, Marks LS, Margolis DJ, Huang J, Macairan ML, Lieu P, Fenster A (2011) Clinical application of a 3D ultrasound-guided prostate biopsy system. *Urol Oncol* 29(3):334–342. <https://doi.org/10.1016/j.urolonc.2011.02.014>
- Sonn GA, Natarajan S, Margolis DJ, MacAiran M, Lieu P, Huang J, Dorey FJ, Marks LS (2013) Targeted biopsy in the detection of prostate cancer using an office based magnetic resonance ultrasound fusion device. *J Urol* 189(1):86–91. <https://doi.org/10.1016/j.juro.2012.08.095>
- Moore CM, Kasivisvanathan V, Eggener S, Emberton M, Futterer JJ, Gill IS, Grubb Iii RL, Hadaschik B, Klotz L, Margolis DJ, Marks LS, Melamed J, Oto A, Palmer SL, Pinto P, Puech P, Punwani S, Rosenkrantz AB, Schoots IG, Simon R, Taneja SS, Turkbey B, Ukimura O, van der Meulen J, Villers A, Watanabe Y, Consortium S (2013) Standards of reporting for MRI-targeted biopsy studies (START) of the prostate: recommendations from an International Working Group. *Eur Urol* 64(4):544–552. <https://doi.org/10.1016/j.eururo.2013.03.030>
- Calio B, Sidana A, Sugano D, Gaur S, Jain A, Maruf M, Xu S, Yan P, Kruecker J, Merino M, Choyke P, Turkbey B, Wood B, Pinto P (2017) Changes in prostate cancer detection rate of MRI-TRUS fusion vs systematic biopsy over time: evidence of a learning curve. *Prostate Cancer Prostatic Dis*. <https://doi.org/10.1038/pcan.2017.34>
- Gaziev G, Wadhwa K, Barrett T, Koo BC, Gallagher FA, Serrao E, Frey J, Seidenader J, Carmona L, Warren A, Gnanapragasam V, Doble A, Kastner C (2016) Defining the learning curve for multiparametric magnetic resonance imaging (MRI) of the prostate using MRI-transrectal ultrasonography (TRUS) fusion-guided



- transperineal prostate biopsies as a validation tool. *BJU Int* 117(1):80–86. <https://doi.org/10.1111/bju.12892>
21. Le Nobin J, Rosenkrantz AB, Villers A, Orczyk C, Deng FM, Melamed J, Mikheev A, Rusinek H, Taneja SS (2015) Image guided focal therapy for magnetic resonance imaging visible prostate cancer: defining a 3-dimensional treatment margin based on magnetic resonance imaging histology co-registration analysis. *J Urol* 194(2):364–370. <https://doi.org/10.1016/j.juro.2015.02.080>
  22. de Gorski A, Roupret M, Peyronnet B, Le Cossec C, Granger B, Comperat E, Cussenot O, Renard-Penna R, Mozer P (2015) Accuracy of magnetic resonance imaging/ultrasound fusion targeted biopsies to diagnose clinically significant prostate cancer in enlarged compared to smaller prostates. *J Urol* 194(3):669–673. <https://doi.org/10.1016/j.juro.2015.03.025>